The Antibiotic Thermorubin Inhibits Protein Synthesis by Binding to Inter-Subunit Bridge B2a of the Ribosome

ARTICLE *in* JOURNAL OF MOLECULAR BIOLOGY · MARCH 2012

Impact Factor: 4.33 · DOI: 10.1016/j.jmb.2011.12.055 · Source: PubMed

3 AUTHORS, INCLUDING:

David Bulkley
Yale University
10 PUBLICATIONS **209** CITATIONS
SEE PROFILE

Francis Johnson
Stony Brook University
252 PUBLICATIONS **6,962** CITATIONS
SEE PROFILE

doi:10.1016/j.jmb.2011.12.055 J. Mol. Biol. (2012) 416, 571–578

Contents lists available at www.sciencedirect.com

Journal of Molecular Biology

journal homepage: http://ees.elsevier.com.jmb

The Antibiotic Thermorubin Inhibits Protein Synthesis by Binding to Inter-Subunit Bridge B2a of the Ribosome

David Bulkley[1], Francis Johnson[2] and Thomas A. Steitz[1,3,4*]

[1]*Department of Chemistry, Yale University, 225 Prospect Street, PO Box 208107, New Haven, CT 06520-8107, USA*
[2]*Department of Pharmacological Sciences, School of Medicine, Stony Brook University, Stony Brook, NY 11794-8651, USA*
[3]*Department of Molecular Biophysics and Biochemistry, Yale University, 260 Whitney Avenue, PO Box 208114, New Haven, CT 06520-8114, USA*
[4]*Howard Hughes Medical Institute, New Haven, CT 06511, USA*

Received 19 October 2011; received in revised form 13 December 2011; accepted 27 December 2011
Available online 2 January 2012

Edited by J. Doudna

Keywords:
ribosome;
translation inhibitor;
antibiotic;
thermorubin;
crystal structure

Thermorubin is a small-molecule inhibitor of bacterial protein synthesis, but relatively little is known about the molecular mechanism by which it blocks translation. The structure of the complex between thermorubin and the 70S ribosome from *Thermus thermophilus* reported here shows that thermorubin interacts with the ribosome in a way that is distinct from any other known class of ribosome inhibitor. Though it is structurally similar to tetracycline, it binds to the ribosome at an entirely different location—the interface between the small and large subunits that is formed by inter-subunit bridge B2a. This region of the ribosome is known to play a role in the initiation of translation, and thus, the binding site we observe is consistent with evidence suggesting that thermorubin inhibits the initiation stage of protein synthesis. The binding of thermorubin induces a rearrangement of two bases on helix 69 of the 23S rRNA, and presumably, this rearrangement blocks the binding of an A-site tRNA, thereby inhibiting peptide bond formation. Due in part to its low solubility in aqueous media, thermorubin has not been used clinically, although it is a potent antibacterial agent with low toxicity (Therapeutic Index > 200). The interactions between thermorubin and the ribosome, as well as its adjacency to the observed binding sites of three other antibiotic classes, may enable the design of novel derivatives that share thermorubin's mode of action but possess improved pharmacodynamic properties.

Introduction

Small-molecule inhibitors of bacterial protein synthesis are widely used as antibiotics.[1] In part because of misuse of these agents, drug-resistant bacteria eventually arise for each antibiotic, necessitating the development of new antibiotics.[2] Unfortunately, drug discovery has not kept pace with the increase in bacterial resistance, and the current need for new antibiotics to treat infectious diseases, especially those of nosocomial origin, is outstripping supply.[3] Thus, identifying new ways to target bacterial protein synthesis may lead to the creation of new antibiotics that are capable of addressing this issue. Here, we show that the little-studied antibiotic thermorubin binds to the 70S ribosome from *Thermus thermophilus* in a way that is distinct from related ribosomal inhibitors but adjacent to the binding sites of different families of antibiotics, thus

*Corresponding author. Department of Chemistry, Yale University, 225 Prospect Street, PO Box 208107, New Haven, CT 06520-8107, USA. E-mail address: thomas.steitz@yale.edu.

Abbreviations used: MIC, minimum inhibitory concentration; PDB, Protein Data Bank.

Table 1. Data collection and refinement statistics for 70S·thermorubin complex

Data collection	
Space group	$P2_12_12_1$
Cell dimensions	
a, *b*, *c* (Å)	210.1, 449.4, 621.7
Resolution (Å)	50–3.2 (3.28–3.20)
R_{mrgd} (%)	20.7 (87.0)
$I/\sigma I$	9.09 (1.92)
Completeness (%)	99.9 (99.9)
Redundancy	7.6 (7.3)
Refinement	
R_{work} (%)	24.3
R_{free} (%)	27.2
Bond rmsd (Å)	0.010
Angle rmsd (°)	1.14

opening up the possibility of developing new antibiotic compounds.

Thermorubin is a natural product that was isolated from *Thermoactinomyces antibioticus*, a thermophilic actinomycete that grows best at ~50 °C.[4] Besides having antibiotic properties, it has also been shown to be a potent aldose reductase inhibitor.[5] Its mechanism of action as an antibiotic is the inhibition of protein synthesis in both Gram-positive and Gram-negative bacteria, but it is inactive against yeast, fungi and higher eukaryotes.[6] Relatively strong activity has been reported against several bacteria, including *Staphylococcus aureus* [minimum inhibitory concentration (MIC) = 0.006 μg/mL], *Streptococcus pyogenes* (MIC = 0.025 μg/mL) and *Streptococcus pneumonia* (MIC = 0.05 μg/mL).[7] Its structure bears a superficial resemblance to that of the tetracyclines since its core is a linear tetracycle, but it differs in being a totally aromatic anthracenopyranone; surprisingly, it does not contain a single chiral center. Unlike the tetracyclines, thermorubin binds to both the large and the small ribosomal subunits with roughly equal affinity (K_d = 1–2 μM) but binds 100-fold more tightly to the full 70S particle,[8] suggesting a single high-affinity binding site on the 70S assembly that is formed by two separate contributions from regions on the large and small subunits. Thermorubin is also capable of chelating two magnesium ions under intracellular ionic concentrations.

Thermorubin is able to inhibit protein synthesis, but only under certain conditions. First, it does not inhibit poly(U)-directed poly(Phe) synthesis at low magnesium concentrations (5 mM) or in the absence of initiation factors[6] nor does it affect the reactivity of puromycin with the 70S ribosome complex with AcPhe-tRNA and poly(U).[9] However, when initiation factors are also present, thermorubin inhibits both poly(U)-directed poly(Phe) synthesis and the binding of fMet-tRNA to the 70S ribosome.[6] Interestingly, it is also able to block poly(U)-directed poly(Phe) synthesis when the magnesium concentration is raised to 12 mM.[9] Finally, thermorubin promotes subunit association at magnesium concentrations that ordinarily promote subunit dissociation.[8]

We have determined the crystal structure of thermorubin in complex with the 70S ribosome from *T. thermophilus* and observe that it binds to the ribosome in the vicinity of inter-subunit bridge B2a and near the binding sites of several other ribosomal inhibitors.[10–12] However, thermorubin binds in a way that is distinct from these other compounds and causes a unique conformational change in the ribosomal RNA. This, combined with the fact that thermorubin apparently targets the initiation stage of protein synthesis, has led us to conclude that the mechanism by which thermorubin inhibits protein synthesis is functionally different from these previously studied compounds.

Results

We determined the co-crystal structure of thermorubin in complex with the 70S ribosome from *T. thermophilus* at 3.2 Å resolution, and the resulting statistics are shown in Table 1. The structure was solved by molecular replacement using a model of the 70S ribosome,[13] and refinement was carried out using the PHENIX package.[14] Coordinates for thermorubin were withheld during refinement of the structure, and an unbiased $F_o - F_c$ difference Fourier electron density map was used to position the small-molecule crystal structure of thermorubin[15] on the 70S ribosome.

Thermorubin interacts with both the large and the small subunits

We observe that thermorubin interacts with both the large and the small subunits (Fig. 1), which is consistent with available biochemical evidence.[8] The antibiotic binds between helix 69 of the 23S RNA and helix 44 of the 16S RNA in the region of inter-subunit bridge B2a (Fig. 2a). This binding site,

Fig. 1. Interactions between thermorubin and the ribosome. (a) An unbiased $F_o - F_c$ difference Fourier map of thermorubin in complex with the *T. thermophilus* 70S ribosome. The difference electron density is contoured at 3 σ, with the corresponding model for thermorubin shown in yellow; oxygen atoms, in red; and two putative ions, as gray spheres. (b) The chemical structure of thermorubin with the positions of various oxygen atoms numbered. The diagram also shows interactions between the drug and cations as well as nucleotides of the ribosomal RNA. (c) Detailed view of the binding site of thermorubin. The antibiotic is shown in yellow, with residues of the 16S RNA shown in beige and with residues of the 23S RNA shown in purple.

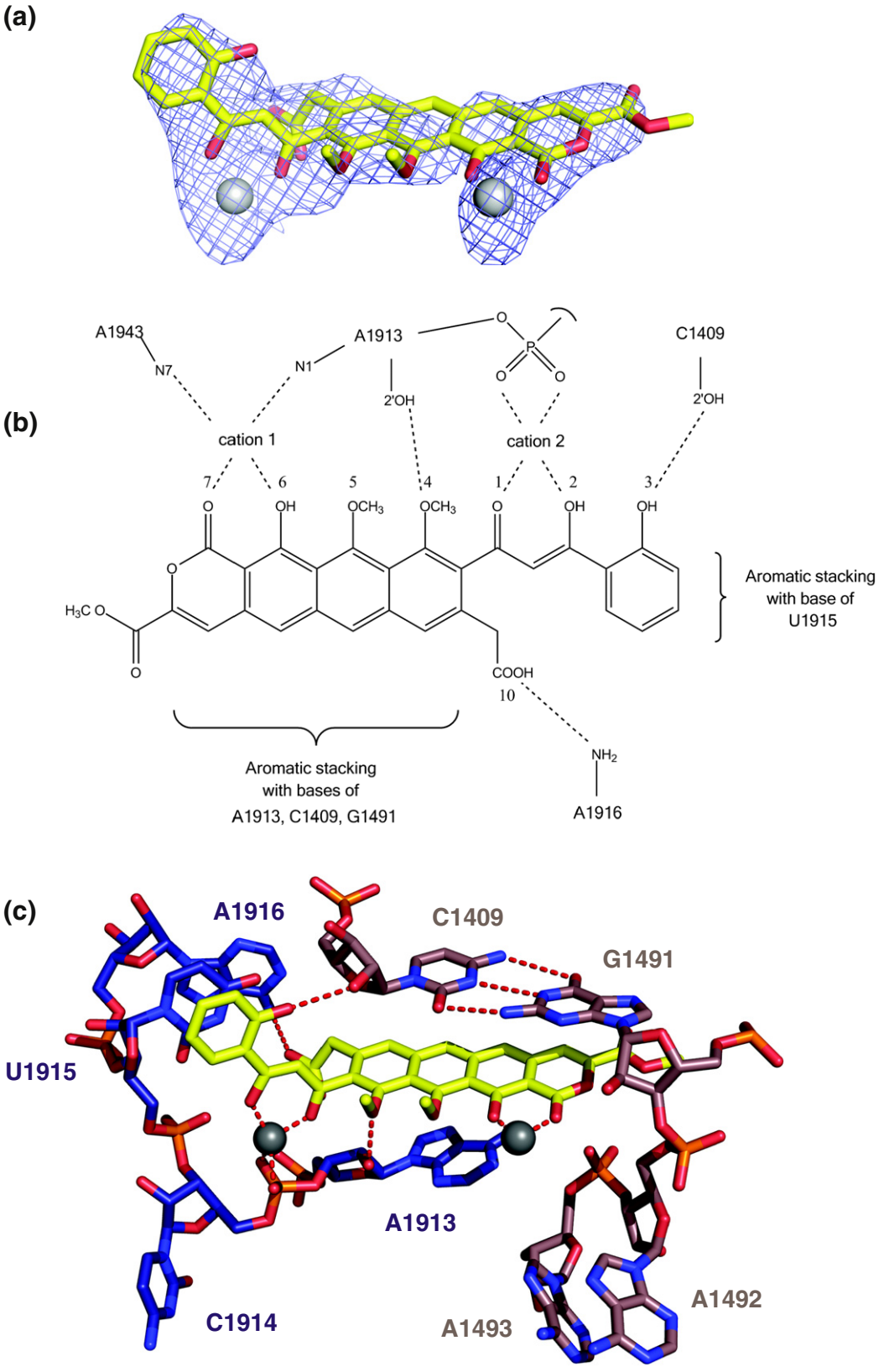

Fig. 1 (*legend on previous page*)

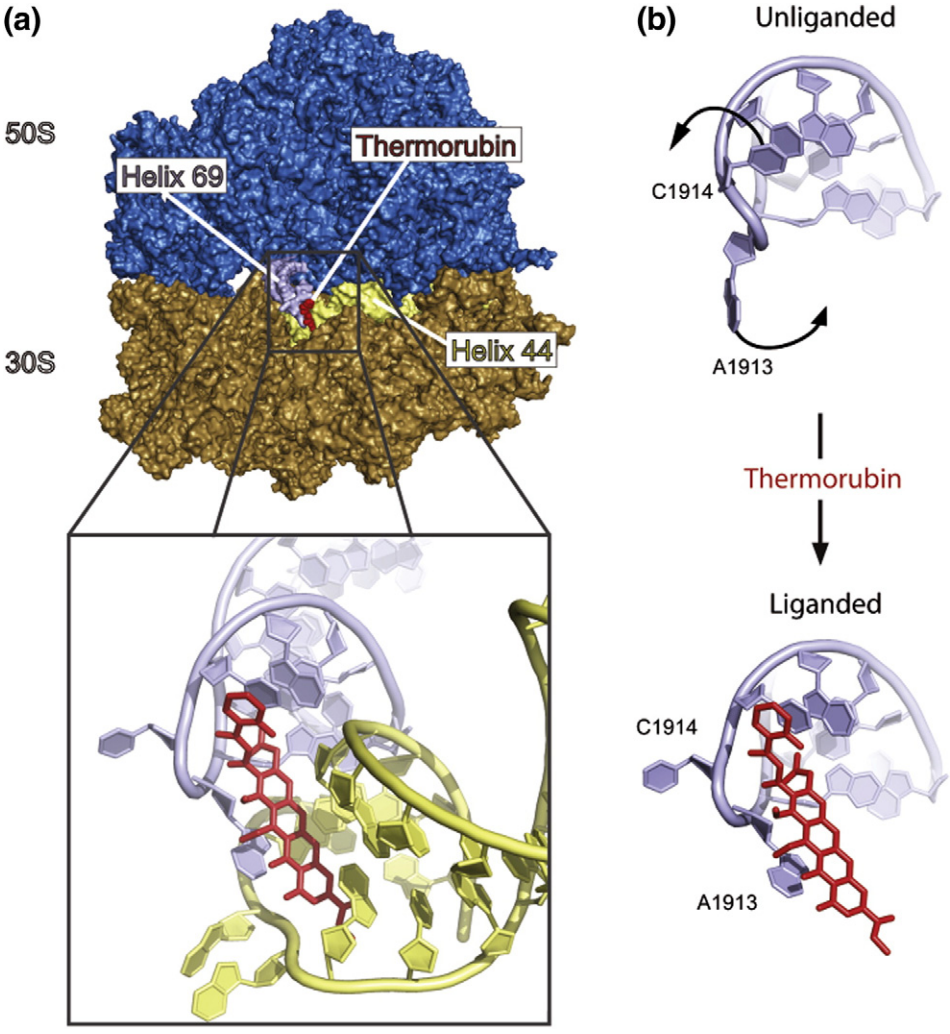

Fig. 2. The binding site of thermorubin. (a) An overview of the ribosome in complex with thermorubin. The large subunit is shown in blue, and the small subunit is shown in gold, with thermorubin shown in red. A close-up view of thermorubin bound to the ribosome shows that the drug nestled between helix 69 (blue gray) of the large subunit and helix 44 (yellow) of the small subunit. (b) Conformational changes in residues C1914 and A1913 of helix 69 of the large ribosomal subunit induced by the binding of thermorubin. The "unliganded" helix 69 shown above is taken from a structure of the complex between aminoacylated tRNA, paromomycin and the 70S ribosome (PDB code 2WDI).[11] The "liganded" helix 69 shown below is the complex between thermorubin and the 70S ribosome.

which is shared equally between both subunits, explains why thermorubin is able to bind either the large or the small subunit individually, as well as the full 70S particle. The tetracyclic moiety of thermorubin stacks against the bases of C1409 and G1491 of the small subunit and A1913 of the large subunit (Fig. 1). The base of U1915 of the 23S RNA supplies an additional stacking interaction with the drug's orthohydroxyphenyl moiety. Residues C1409 and A1913 also appear to form hydrogen bonds with the antibiotic at oxygens 3 and 4 via their 2′-hydroxyl groups. Finally, our data suggest that two cationic species coordinate the drug, bridging metal chelating sites on the antibiotic and electron-rich regions of the ribosomal RNA. These interactions most likely involve magnesium ions, although the second site is very tightly coordinated and, thus, may not be sufficiently large to accommodate a magnesium ion. The presence of two bound cations is consistent with the observation that thermorubin chelates two magnesium ions in solution.[8]

Rearrangement of the bases of C1914 and A1913

The binding of thermorubin causes conformational changes in the ribosomal RNA that have important functional consequences. The bases of A1913 and C1914 lie at the tip of helix 69 on the 23S RNA, and when thermorubin binds, the bases of these residues are repositioned (Fig. 2b). The adenine at position

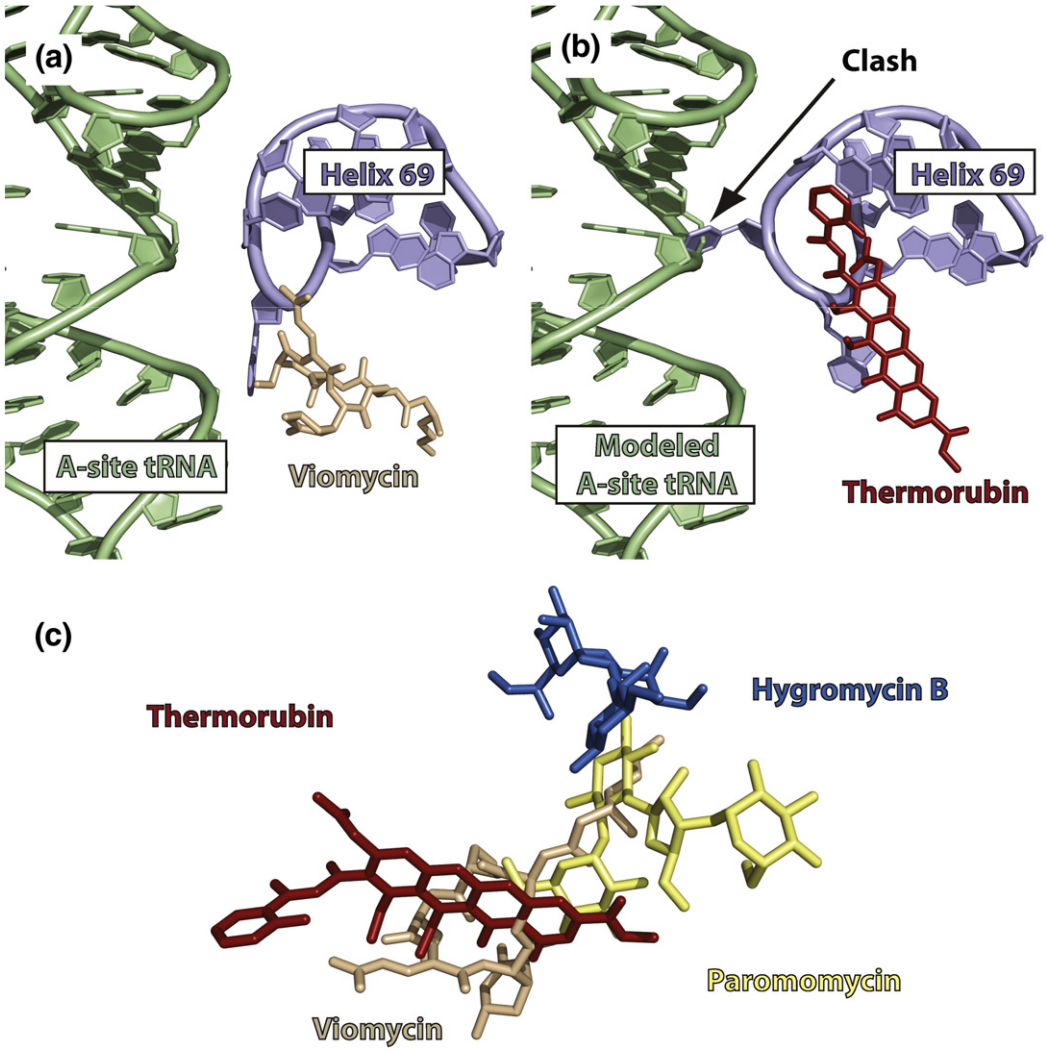

Fig. 3. Comparison between the positions of thermorubin and other antibiotics that bind in the region of inter-subunit bridge B2a. (a) Orientation of helix 69 with A-site tRNA and viomycin in complex with the 70S ribosome (PDB codes 3KNH and 3KNI). The antibiotic viomycin is shown in tan; A-site tRNA, in green; and helix 69, in blue. (b) Orientation of helix 69 when thermorubin is bound. A-site tRNA[11] (PDB 3KNH) is superimposed to show that reorientation of residue C1914 when thermorubin binds would result in a clash between accommodated A-site tRNA and helix 69 of the 23S RNA. (c) Superimposition of thermorubin with viomycin[11] (PDB 3KNH), paromomycin[10] (PDB 2WDG) and hygromycin B[12] (PDB 3DF1), other antibiotics that bind in the vicinity of inter-subunit bridge B2a. Each structure was superimposed using the phosphate backbone of the 16S RNA in the program LSQMAN.[17]

1913 moves up toward thermorubin's binding site and stacks against the aromatic tetracycle of the antibiotic. Also, the coordination of the N1 of A1913 with the magnesium ion that is bound by oxygens 6 and 7 of thermorubin further stabilizes this rearrangement. A slight movement of the sugar at position 1913 also takes place, facilitated by the formation of a hydrogen bond between the 2′-OH on the ribose sugar and oxygen 4 of thermorubin. While A1913 moves toward thermorubin, C1914 is pushed away. The base of C1914 ordinarily stacks against the base of U1915,[10,13,16] but the terminal orthohydroxyphenyl moiety of the drug displaces the base of C1914 from its stacking interaction and forms a hydrogen bond with the 2′-hydroxyl on the ribose sugar of C1409 via oxygen 3. With this position blocked, the base of C1914 rotates out, away from the central axis of helix 69 and into the region normally occupied by a bound A-site tRNA (Fig. 3b).

Discussion

Our observation that the conformational change produced by the binding of thermorubin is likely to block the binding of an A-site tRNA is consistent

with biochemical evidence suggesting that the binding of thermorubin to the 70S ribosome blocks the initiation phase of bacterial protein synthesis. Thermorubin has relatively little effect on *in vitro* poly(U)-dependent poly-phenylalanine synthesis, a process that bypasses the normal route of translation initiation,[6,9] whereas thermorubin effectively inhibits the *in vitro* translation of an endogenous mRNA containing a start codon and a Shine–Dalgarno sequence.[6] While poly(U)-dependent poly-phenylalanine synthesis is not inhibited by thermorubin under physiological magnesium concentrations (6 mM), the drug is able to block poly-phenylalanine synthesis under elevated magnesium concentrations (12 mM).[9] Interestingly, the level of inhibition that can be achieved depends on whether thermorubin is introduced before or after poly(U) is added to the system. Prior incubation of 70S particles with thermorubin leads to near-complete inhibition of poly-phenylalanine synthesis, while simultaneous addition of poly(U) and thermorubin leads only to a 30% reduction in poly-phenylalanine synthesis even at the highest concentrations of thermorubin. The structure of the complex between thermorubin and the 70S ribosome suggests that an A-site tRNA and thermorubin could not simultaneously occupy the ribosome (Fig. 3b). Thus, it may be that thermorubin preferentially binds during the initiation phase because a ribosome at this stage of protein synthesis is more likely to have an A-site that is vacant of tRNA.

It has also been observed that thermorubin is able to prevent initiator tRNA from binding to the *Escherichia coli* ribosome when initiation factors are present.[9] The region of the ribosome at which thermorubin binds, inter-subunit bridge B2a (Fig. 2a), has been shown to play a role in factor-dependent translation initiation,[18,19] and IF1 and IF2 have been observed to make contacts with this region.[20–23] Both C1914 and A1913 lie adjacent to IF2 when it is bound in a 70S initiation complex, and both of these bases are repositioned by the binding of thermorubin. Thus, the rearrangement of C1914 and A1913 may alter the interaction between bridge B2a and initiation factors in such a way that the binding of initiator tRNA in the P-site is blocked. From the structure presented here, it is clear that thermorubin alone would have relatively little effect on the accommodation of a P-site tRNA during translation initiation. Instead, our data show that the binding of thermorubin repositions the base of C1914 of the 23S RNA into the A-site, which would clash with an accommodated A-site tRNA, not an initiator tRNA in the P-site. As we do not know exactly which stage of initiation thermorubin inhibits, it is also possible that fMet-tRNA is accommodated in the P-site, but it is the decoding of the first A-site-bound tRNA that is inhibited. Bridge B2a is dispensable for *in vitro* protein synthesis, but its removal by deletion or mutation of helix 69 is lethal to *E. coli* cells,[24,25] raising the possibility that thermorubin interferes with another aspect of bridge B2a function by binding to this region of the ribosome.

In addition to its role in translation initiation, bridge B2a links the large and small subunits during inter-subunit ratcheting, which occurs during the elongation phase of protein synthesis.[26] Thermorubin binds in a cleft formed by helix 69 and helix 44 at the edge of bridge B2a and could be expected to increase the stability of this region of the inter-subunit bridge. It has been shown that bridge B2a undergoes at least a 7-Å movement during ratcheting,[27] and it is possible that thermorubin prevents this motion by rigidifying the link between helix 69 and helix 44. Two observations support this idea. The first is that thermorubin prevents dissociation of the 70S ribosome into subunits.[15] Second, thermorubin inhibits protein synthesis at higher magnesium concentrations (above 12 mM),[9] suggesting that the combined stabilizing effects of high magnesium and thermorubin cooperatively block translation by limiting inter-subunit mobility.

While thermorubin is a potent inhibitor of ribosomes from both Gram-positive and Gram-negative bacteria, it is essentially inactive against ribosomes from yeast, fungi[4] and higher eukaryotes.[7] This specificity is explained by the differences in the structures of the eukaryotic and prokaryotic ribosomal RNAs that form the thermorubin binding site. Upon binding to the bacterial ribosome, the tetracyclic aromatic region of thermorubin stacks against the bases of C1409 and G1491, which form a Watson–Crick base pair (Fig. 1). In the yeast 80S ribosome, the equivalent bases C1646 and A1754 are not capable of forming a Watson–Crick base pair, suggesting that they may not be able to accommodate thermorubin. Examination of the crystal structure of the yeast 80S ribosome reveals that A1754 base pairs with U1647 (one residue above C1646, the equivalent of *E. coli* base C1409) and, thereby, eliminates the long, flat, aromatic surface against which thermorubin packs when bound to the prokaryotic ribosome.[28] It would be interesting to see whether mutation of G1491 to an adenosine in *E. coli* would render the bacterial ribosome resistant to thermorubin. Because thermorubin may depend on initiation factors to inhibit protein synthesis, it is possible that its prokaryotic specificity is also a result of differences between how prokaryotic and eukaryotic translation initiation factors interact with the ribosome.

Despite its potency against a variety of Gram-positive and Gram-negative bacteria *in vitro*, thermorubin is relatively ineffective in the treatment of bacterial infections when administered orally or intravenously.[7] It is likely that the compound's limited solubility in aqueous solution prevents it

from reaching the site of infection, given that thermorubin is effective against *S. pyogenes* only when administered intraperitoneally.[4] Consequently, chemical modifications of thermorubin will be necessary to improve its pharmacokinetic characteristics to enable the compound to be used clinically. The location of thermorubin next to the binding sites of three other families of antibiotics[10–12] identifies and further extends a contiguous antibiotic binding surface that can be used for the structure-based design of novel antibacterial substances (Fig. 3c). Perhaps, a completely *de novo* drug could be designed to target the large ribosomal surface seen to bind these four antibiotics; a similar strategy is being implemented successfully by Rib-X Pharmeceuticals[29] to obtain a new antibiotic class that targets the bacterial peptidyl transferase center.[30]

Materials and Methods

Thermorubin was isolated from *T. antibioticus* as reported previously.[4] 70S ribosomes from *T. thermophilus* were purified and crystallized according to previously published work, with minor adjustments in the crystallization procedure.[31] Briefly, purified 70S ribosomes were diluted to 10 mg/mL in buffer composed of 5 mM Hepes (pH 7.5), 50 mM KCl, 10 mM NH_4Cl and 10 mM $MgAc_2$ and then equilibrated via sitting-drop vapor diffusion against a reservoir solution made up of 2.9% (w/v) polyethylene glycol 20,000, 9% (v/v) methyl-2,4-pentanediol, 175 mM L-arginine and 100 mM Tris–HCl (pH 7.6). Immediately prior to equilibration, the ribosome-containing solution was mixed in a ratio of 3:4, ribosome to reservoir solution. Crystals appeared after approximately 4 days and were harvested after 8 days. Following stabilization by gradually increasing the concentration of 2-methyl-2,4-pentanediol to 40% (v/v), thermorubin was added to the mother liquor at a concentration of 100 μM. After 12 h of equilibration, the crystals were flash frozen in a nitrogen cryostream at 80 °K. Diffraction data were collected at the National Synchrotron Light Source on beamline X-25 using a Pilatus 6 M detector. Data reduction was performed with the program XDS,[32] and an initial solution was generated by molecular replacement with Phaser[33] using the *T. thermophilus* 70S ribosome as a search model.[13] The solution was then refined with the PHENIX package.

Accession numbers

Atomic coordinates were deposited under Protein Data Bank (PDB) accession numbers 3UXQ, 3UXR, 3UXS and 3UXT.

Acknowledgements

This work was supported by the National Institutes of Health grant GM022778 awarded to T.A.S. We would like to thank David Keller for his help with crystal freezing and cryoprotection and the beamlines at the Brookhaven National Laboratory (X-29 and X-25) for the use of their facilities and technical assistance with data collection. We thank the Yale Center for Structural Biology staff, particularly Michael Strickler, for assistance with data processing and Gregor Blaha and C. Axel Innis for helpful discussions during manuscript preparation.

References

1. Wilson, D. N. (2009). The A–Z of bacterial translation inhibitors. *Crit. Rev. Biochem. Mol. Biol.* **44**, 393–433.
2. Chen, L. F., Chopra, T. & Kaye, K. S. (2011). Pathogens resistant to antibacterial agents. *Med. Clin. North Am.* **95**, 647–676.
3. Freire-Moran, L., Aronsson, B., Manz, C., Gyssens, I. C., So, A. D., Monnet, D. L. & Cars, O. (2011). Critical shortage of new antibiotics in development against multidrug-resistant bacteria—time to react is now. *Drug Resist. Updat.* **14**, 118–124.
4. Craveri, R., Coronelli, C., Pagani, H. & Sensi, P. (1964). Thermorubin, a new antibiotic from a thermoactinomycete. *Clin. Med. (Northfield Il)*, **71**, 511–521.
5. Hayashi, K., Dombou, M., Sekiya, M., Nakajima, H., Fujita, T. & Nakayama, M. (1995). Thermorubin and 2-hydroxyphenyl acetic acid, aldose reductase inhibitors. *J. Antibiot. (Tokyo)*, **48**, 1345–1346.
6. Pirali, G., Somma, S., Lancini, G. C. & Sala, F. (1974). Inhibition of peptide chain initiation in *Escherichia coli* by thermorubin. *Biochim. Biophys. Acta*, **366**, 310–318.
7. Cavalleri, B., Turconi, M. & Pallanza, R. (1985). Synthesis and antibacterial activity of some derivatives of the antibiotic thermorubin. *J. Antibiot. (Tokyo)*, **38**, 1752–1760.
8. Lin, F. & Wishnia, A. (1982). The protein synthesis inhibitor thermorubin. 1. Nature of the thermorubin–ribosome complex. *Biochemistry*, **21**, 477–483.
9. Lin, F. & Wishnia, A. (1982). The protein synthesis inhibitor thermorubin. 2. Mechanism of inhibition of initiation on *Escherichia coli* ribosomes. *Biochemistry*, **21**, 484–491.
10. Voorhees, R. M., Weixlbaumer, A., Loakes, D., Kelley, A. C. & Ramakrishnan, V. (2009). Insights into substrate stabilization from snapshots of the peptidyl transferase center of the intact 70S ribosome. *Nat. Struct. Mol. Biol.* **16**, 528–533.
11. Stanley, R. E., Blaha, G., Grodzicki, R. L., Strickler, M. D. & Steitz, T. A. (2010). The structures of the anti-tuberculosis antibiotics viomycin and capreomycin bound to the 70S ribosome. *Nat. Struct. Mol. Biol.* **17**, 289–293.
12. Borovinskaya, M. A., Shoji, S., Fredrick, K. & Cate, J. H. (2008). Structural basis for hygromycin B inhibition of protein biosynthesis. *RNA*, **14**, 1590–1599.
13. Selmer, M., Dunham, C. M., Murphy, F. V., IV, Weixlbaumer, A., Petry, S., Kelley, A. C. *et al.* (2006). Structure of the 70S ribosome complexed with mRNA and tRNA. *Science*, **313**, 1935–1942.
14. Adams, P. D., Afonine, P. V., Bunkoczi, G., Chen, V. B., Davis, I. W., Echols, N. *et al.* (2010). PHENIX: a

comprehensive Python-based system for macromolecular structure solution. *Acta Crystallogr., Sect. D: Biol. Crystallogr.* **66**, 213–221.
15. Johnson, F., Chandra, B., Iden, C. R., Naiksatam, P., Kahen, R., Okaya, Y. & Lin, S. (1980). Thermorubin. 1. Structure studies. *J. Am. Chem. Soc.* **102**, 5580–5585.
16. Zhang, W., Dunkle, J. A. & Cate, J. H. (2009). Structures of the ribosome in intermediate states of ratcheting. *Science*, **325**, 1014–1017.
17. Kleywegt, G. J. & Jones, T. A. (1994). Detection, delineation, measurement and display of cavities in macromolecular structures. *Acta Crystallogr., Sect. D: Biol. Crystallogr.* **50**, 178–185.
18. Kipper, K., Hetenyi, C., Sild, S., Remme, J. & Liiv, A. (2009). Ribosomal intersubunit bridge B2a is involved in factor-dependent translation initiation and translational processivity. *J. Mol. Biol.* **385**, 405–422.
19. Hirabayashi, N., Sato, N. S. & Suzuki, T. (2006). Conserved loop sequence of helix 69 in *Escherichia coli* 23 S rRNA is involved in A-site tRNA binding and translational fidelity. *J. Biol. Chem.* **281**, 17203–17211.
20. Marzi, S., Knight, W., Brandi, L., Caserta, E., Soboleva, N., Hill, W. E. *et al.* (2003). Ribosomal localization of translation initiation factor IF2. *RNA*, **9**, 958–969.
21. Allen, G. S., Zavialov, A., Gursky, R., Ehrenberg, M. & Frank, J. (2005). The cryo-EM structure of a translation initiation complex from *Escherichia coli*. *Cell*, **121**, 703–712.
22. Myasnikov, A. G., Marzi, S., Simonetti, A., Giuliodori, A. M., Gualerzi, C. O., Yusupova, G. *et al.* (2005). Conformational transition of initiation factor 2 from the GTP- to GDP-bound state visualized on the ribosome. *Nat. Struct. Mol. Biol.* **12**, 1145–1149.
23. Carter, A. P., Clemons, W. M., Jr, Brodersen, D. E., Morgan-Warren, R. J., Hartsch, T., Wimberly, B. T. & Ramakrishnan, V. (2001). Crystal structure of an initiation factor bound to the 30S ribosomal subunit. *Science*, **291**, 498–501.
24. Ali, I. K., Lancaster, L., Feinberg, J., Joseph, S. & Noller, H. F. (2006). Deletion of a conserved, central ribosomal intersubunit RNA bridge. *Mol. Cell*, **23**, 865–874.
25. Liiv, A., Karitkina, D., Maivali, U. & Remme, J. (2005). Analysis of the function of *E. coli* 23S rRNA helix–loop 69 by mutagenesis. *BMC Mol. Biol.* **6**, 18.
26. Frank, J. & Agrawal, R. K. (2000). A ratchet-like intersubunit reorganization of the ribosome during translocation. *Nature*, **406**, 318–322.
27. Dunkle, J. A., Wang, L., Feldman, M. B., Pulk, A., Chen, V. B., Kapral, G. J. *et al.* (2011). Structures of the bacterial ribosome in classical and hybrid states of tRNA binding. *Science*, **332**, 981–984.
28. Ben-Shem, A., Jenner, L., Yusupova, G. & Yusupov, M. (2010). Crystal structure of the eukaryotic ribosome. *Science*, **330**, 1203–1209.
29. Franceschi, F. & Duffy, E. M. (2006). Structure-based drug design meets the ribosome. *Biochem. Pharmacol.* **71**, 1016–1025.
30. Skripkin, E., McConnell, T. S., DeVito, J., Lawrence, L., Ippolito, J. A., Duffy, E. M. *et al.* (2008). Rχ-01, a new family of oxazolidinones that overcome ribosome-based linezolid resistance. *Antimicrob. Agents Chemother.* **52**, 3550–3557.
31. Bulkley, D., Innis, C. A., Blaha, G. & Steitz, T. A. (2010). Revisiting the structures of several antibiotics bound to the bacterial ribosome. *Proc. Natl Acad. Sci. USA*, **107**, 17158–17163.
32. Kabsch, W. (2010). XDS. *Acta Crystallogr., Sect. D: Biol. Crystallogr.* **66**, 125–132.
33. McCoy, A. J., Grosse-Kunstleve, R. W., Adams, P. D., Winn, M. D., Storoni, L. C. & Read, R. J. (2007). Phaser crystallographic software. *J. Appl. Crystallogr.* **40**, 658–674.